Non-invasive super-resolution imaging through dynamic scattering media

Dong Wang
Nanyang Technological University
Sujit Sahoo
Indian Institute of Technology Goa https://orcid.org/0000-0002-1208-9466
Xiangwen Zhu
Nanyang Technological University (NTU) https://orcid.org/0000-0002-7535-4511
Giorgio Adamo
Nanyang Technological University
Cuong Dang (hcdang@ntu.edu.sg)
Nanyang Technological University (NTU) https://orcid.org/0000-0001-6183-4082

Article

Keywords: super-resolution imaging, scattering media, biological tissue, decorrelation, stochastic, localization

Posted Date: November 19th, 2020

DOI: https://doi.org/10.21203/rs.3.rs-104907/v1

Version of Record: A version of this preprint was published at Nature Communications on May 25th, 2021. See the published version at https://doi.org/10.1038/s41467-021-23421-4.

Non-invasive super-resolution imaging through dynamic scattering media

Dong Wang [1,2,#], Sujit K. Sahoo[1,3,#], Xiangwen Zhu[1], Giorgio Adamo[4] and Cuong Dang[1,*]

[1] Centre for Optoelectronics and Biophotonics (COEB), School of Electrical and Electronic Engineering, The Photonics Institute (TPI), Nanyang Technological University Singapore, 50 Nanyang Avenue, 639798, Singapore

[2] Key Laboratory of Advanced Transducers and Intelligent Control System, Ministry of Education, and Shanxi Province, College of Physics and Optoelectronics, Taiyuan University of Technology, Taiyuan 030024, China

[3] School of Electrical Sciences, Indian Institute of Technology Goa, Goa 403401, India

[4] Centre for Disruptive Photonic Technologies, SPMS, TPI, Nanyang Technological University, Singapore 637371, Singapore

[#] Dong Wang and Sujit K. Sahoo contribute equally.

*Corresponding author, E-mail: HCDang@ntu.edu.sg

Keywords: super-resolution imaging, scattering media, biological tissue, decorrelation, stochastic, localization

Abstract

Super-resolution imaging has been revolutionizing technical analysis in various fields from biological to physical sciences. However, many objects are hidden by strongly scattering media such as biological tissues that scramble light paths, create speckle patterns and hinder object's visualization, let alone super-resolution imaging. Here, we demonstrate non-invasive super-resolution imaging through scattering media based on a stochastic optical scattering localization imaging (SOSLI) technique. After capturing multiple speckle patterns of photo-switchable emitters, our stochastic approach utilizes the speckle correlation property of scattering media to retrieve an image with 100-nm resolution, eight-fold enhancement compared to the diffraction limit. More importantly, we demonstrate our SOSLI to do non-invasive super-resolution imaging through not only static scattering media, but also dynamic scattering media with strong decorrelation such as biological tissues. Our approach paves the way to non-invasively visualize various samples behind scattering media at unprecedented levels of detail.

Introduction

Optical imaging beyond diffraction-limit resolution has enabled incredible tools to advance science and technology from investigation of the interior of biological cells[1,2] to chemical reactions at single molecule levels[3]. Super-resolution stimulated emission

depletion (STED) microscopy[4] has progressed rapidly to achieve three-dimensional (3D) imaging with super-high spatiotemporal precision[5,6]. For single-molecule detection and localization approaches[7,8], such as stochastic optical reconstruction microscopy (STORM) or photo-activated localization microscopy (PALM), positions of photo-switchable probes are determined as centers of diffraction-limited spots. Repeating multiple imaging processes, each with a stochastically different subset of active fluorophores, allows nanometer-resolution image reconstruction[9]. After these pioneering techniques, the field of super-resolution microscopy has developed rapidly with various other techniques[10-12] to bring the optical microscopy within the resolution of electron microscopy. However, the requirement of sample transparency makes the super-resolution microscopy techniques impossible to access objects, which are hidden by strongly scattering media such as biological tissues, frosted glass, or around rough wall corners (Fig. 1a and supplementary Fig. S1, S2). These media do not absorb light significantly; however, they scramble the light path, create noise-like speckle patterns[13] and challenge even our low-resolution visualization of samples.

Many approaches have been demonstrated to overcome the scattering effects and enabled imaging or focusing capability through scattering media. The most straightforward approaches utilize ballistic photons[14-16]. However, strongly scattering media significantly reduce number of ballistic photons and lower the signal tremendously[17]. Some techniques require a guide star or access to the other side of the scattering media to characterize or reverse their scattering effects before imaging such

as wave-front shaping techniques[18-21] or transfer matrix measurement[22,23]. Another approach relies on memory effect of light through scattering media[24,25] and deconvolution imaging[26-28] because the memory effect implies a shift-invariant point spreading function (PSF). A scattering medium with a known PSF (often being measured invasively) is a scattering lens that, in turn, is a low pass filter like any conventional lens (Fig. 1b and supplementary Fig. S2d-f). Deconvolution imaging currently provides the best-resolution images from speckle patterns with minimum media characterization (single shot PSF measurement). However, each measured PSF is only valid for one scattering medium, therefore, cannot be used for dynamic scattering media. Non-invasive imaging through scattering media where the image is retrieved without characterizing scattering media is desired for real applications. Diffuse optical tomography[29,30] and time-of-flight imaging[14,29,31] are possible solutions, however, with resolution of several orders lower than the optical diffraction limit. Thanks to the shift-invariant speckle-type PSF of thin scattering media, the 2D image and even the 3D image of a sample can be revealed non-invasively from the speckle patterns by a phase retrieval algorithm[32-34]. The limited performance of the algorithm and cameras, together with presence of noise and sample's complexity, usually makes the image retrieval process failed or converged with some artifacts and slightly lower resolution compared to the diffraction limit and certainly to deconvolution images (Fig. 1c and supplementary Fig. S2g-i).

Here, we present our stochastic optical scattering localization imaging (SOSLI)

technique to do non-invasive super-resolution imaging through scattering media. The technique only requires an imaging sensor to capture speckle patterns created by blinking emitters behind a scattering medium (Fig. 1a, Fig. 2a, and supplementary Fig. S1). The positions of emitters in each stochastic frame are determined computationally at very high precision, allowing super-resolution image reconstruction (Fig. 1d). We demonstrate the resolution beyond the diffraction limit by a factor of eight as a proof of concept. While 100-nm feature size behind the scattering media is well resolved in our demonstration, the resolution limit of our SOSLI is determined by signal to noise ratio (SNR), similar to other computational super-resolution microscopy techniques for transparent samples. More interestingly, the localization algorithm is based on a single-shot speckle pattern with minimum correlation amongst adjacent patterns; therefore, we develop adaptive SOSLI to do super-resolution imaging through dynamic scattering media, such as fresh chicken eggshell membranes with decorrelation of up to 80%. Our SOSLI demonstrates a desired technique to see through translucent media such as biological tissues or frosted glass with unprecedented clarity.

Stochastic Optical Scattering Localization Imaging (SOSLI)

An object O consists of stochastically blinking emitters: $O = \sum_{i=1}^{N} O_i$, where O_i is the i^{th} blinking pattern (a subset of O) and N is the total number of the blinking patterns. After light propagating through scattering media, each O_i produces a speckle pattern I_i, captured by a camera (Fig. 2a). If object size is within the memory effect of the scattering media, the PSF is shift-invariant speckles, therefore the speckle pattern I_i

(Fig. 2b) of object O_i preserves the object's autocorrelation[33] (Fig. 2c). The image of O_i can be retrieved from its autocorrelation by an iterative phase retrieval algorithm[33] (Fig. 2d). The limitation in the camera's bit depth, photon budget and performance of phase retrieval algorithms in presence of image acquisition noise degrade the diffraction-limit resolution of this non-invasive retrieval image. However, a standard localization algorithm[35,36] is employed to find the position of emitters at very high resolution (Fig. 2e) and remove algorithm artifacts. Similar to other localization microscopy techniques, the precision is higher for spatially sparse emitter samples where only one emitter is temporally active in a diffraction-limited region. The sharp and clear image O_i' presents the precise relative emitter positions of pattern O_i, while losing their exact positions because O_i' is only retrieved from autocorrelation of O_i through autocorrelation of I_i. The estimated PSF of the scattering medium can be retrieved by deconvolution (Fig. 2f): $PSF' = Deconvol(I_i, O_i')$, which is also shifted in comparison to the actual PSF because of shift in position of O_i' compared to O_i. Besides losing the exact position, phase retrieval algorithm cannot distinguish the true solution with its flip via a central inversion. Therefore, we deduce different PSF' corresponding to different flipped versions of O_i' then validate them in deconvolution with another speckle image (I_j) to determine the correct one. It is worth to note that the phase retrieval algorithm performs better with sparse samples because of not only the simpler solution but also the higher contrast of the speckle image. This phase retrieval solution will affect the subsequence localization and PSF estimation. We should choose the speckle image with highest contrast for phase retrieval and PSF estimation[37].

Next, a series of clean super-resolution images O_j' with emitter positions is reconstructed for a corresponding series of stochastic patterns O_j by deconvolution of its corresponding speckle pattern I_j with the estimated PSF' and localization as presented in Fig. 2g. A super-resolution image of the full sample (Fig. 2h) is now reconstructed by superposing all individual images as: $O' = \sum_{j=1}^{N} O_j'$, which represents object O with an arbitrary position. This principle is valid provided that PSF does not change among the group of I_j. For comparison, we present the typical simulation image (Fig. 2i) retrieved from autocorrelation of a single speckle pattern, in which simulation parameters are similar, with the exception that all the emitters are on. The simulated diffraction limit is about 3.2 pixels. This current state-of-the-art technique for non-invasive imaging through scattering media shows a blurry image (diffraction limit of the optical system) together with some artifacts from the phase retrieval algorithm. In contrast, the image reconstructed by SOSLI is much sharper with single pixel resolution (Fig. 2h).

Super-resolution imaging through a ground glass diffuser

To prove our concept, we first demonstrate SOSLI for non-invasive super-resolution imaging through a ground glass diffuser. Microscopic objects comprising multiple stochastic blinking emitters are created by de-magnifying projector images through a microscope objective. The de-magnifying image of each pixel in a digital micro-mirror device (DMD) is an intermittent emitter with a size of about 1.34 μm (Supplementary Fig. S1a). The microscopic object is placed 10 mm behind the ground glass diffuser,

which is kept unknown in all demonstrations. The incoherent light from the object propagating through the optical diffuser is recorded by a monochromatic camera, which is 100 mm in front of the diffuser. An iris with diameter of 1 mm is placed immediately after the optical diffuser to act as the aperture of the imaging system (Fig. S1b). A larger iris size enhances the diffraction limit of the imaging system and achieves a sharper image (supplementary Fig. S2); however, it reduces the speckle contrast that is vital for phase retrieval approach.

Figure 3 shows the experimental measurements and results for three different imaging approaches. Single-shot non-invasive imaging through scattering media is performed in Fig. 3a-c, where all emitters are on. The image is recovered from the autocorrelation of a single speckle pattern (Fig. 3a) by the phase retrieval algorithm[33]. The image is very blurred, and we cannot distinguish 2 lines with a gap of 4 μm between them (Fig. 3b-c). This is understandable if we calculate the diffraction limit of our system as $0.61\,\lambda/\mathrm{NA} = 6.7\,\mu m$, where λ = 550 nm and NA = 0.05. Beside the diffraction limit, the performance of the phase retrieval algorithm in the presence of experimental noise degrades the image quality and limits the resolution. With the DMD projector, we can measure the PSF by turning on a single pixel at the center only and capture its speckle pattern (Fig. 3d). Such an "invasive guiding star" for the PSF measurement allows us to calculate the image by deconvolution and significantly enhances the resolution (Fig. 3e). The invasive deconvolution approach is more deterministic, robust to the noise and enhances the high spatial frequency components

of the image. We are now able to distinguish the 2 lines with a 4-μm gap, but still cannot see a 2.68-μm gap (Fig. 3e-f). Most strikingly, our super-resolution image reconstructed non-invasively by SOSLI is remarkably clear as presented in Fig. 3g-i. We can resolve very well all the smallest features of our sample, i.e. 2 thin lines (1.34 μm width) with a gap of 1.34 μm in between (Fig. 3h-i). While the smallest sample feature is smaller than the diffraction limit by a factor of 5, Fig. 3h-i clearly illustrates that the capability of our demonstrated SOSLI is far beyond our sample's smallest features, which are currently limited by the projector's pixel size and optics of the sample creating system (Fig. S1a).

It is worth highlighting some important factors in our SOSLI performance. Supplementary Fig. S3 presents more detail for the reconstruction process in which the localization is important in removing all the background noise and artifacts resulting from the phase retrieval algorithm. This leads to a better estimation of PSF for a series of deconvolution calculation after that. Better PSF estimation surely increases the precision of deconvolution and subsequent localization, but SOSLI seems to tolerate more errors in PSF estimation (Supplementary Fig. S4-S5). Our approach relies on stochastic emitter patterns to reconstruct a full object; therefore, the image quality is improved with more stochastic patterns (supplementary Fig. S6). Figure 4 presents some images of more complex objects for performance comparison among the three techniques. Similar to Fig. 3, the complex objects are best resolved with our SOSLI approach (Fig. 4a-c), while the retrieval image from autocorrelation of a single speckle

pattern shows the poorest performance with some artifacts (Fig. 4d-f). The invasive imaging approach by deconvolution shows moderate performance in Fig. 4g-i. Obviously, our SOSLI for non-invasive imaging through scattering media goes far beyond the diffraction limit and surpasses all the current state-of-the-art imaging through scattering media, including both invasive and non-invasive techniques.

Super-resolution imaging through a biological tissue

Our SOSLI demonstrations in Fig. 3 and Fig. 4 rely on a fixed PSF for reconstruction of multiple stochastic emitter patterns; and therefore, we cannot directly use for dynamic scattering media such as biological tissues. Figure 5a shows the decorrelation behaviors of PSFs for two different scattering media. For static scattering media such as a ground glass diffuser, the PSF is a constant pattern and the correlation of 1 is achieved for any measured PSFs at any time. On the other hand, dynamic scattering media such as fresh chicken eggshell membranes, the PSF gradually changes and the correlation with the initial one decreases with time. In our experiment for the fresh chicken eggshell membrane, the correlation reduces from 1.0 to 0.2 after 300 measurements, with the fastest decay rate in the first 70 measurements (correlation decreases to 0.54). For SOSLI, we also measure 300 stochastic patterns in the same condition, so the decorrelation behavior of the membrane is expected to be as the one in Fig. 5a. The reconstruction by SOSLI with a single estimated PSF shows a noisy and blurred image due to this decorrelation (from 1.0 to 0.2) of the membrane as presented in Fig. 5b. Supplementary Fig. S7 presents the deconvolution images from stochastic

speckle patterns with an estimated PSF from the first speckle pattern. Obviously, the assumption of a static PSF in SOSLI does not hold in this case.

We introduce an adaptive approach to demonstrate our SOSLI for super-resolution imaging through dynamic scattering media. We now utilize SOSLI to localize and then superpose emitters in a set of first 50 stochastic patterns, in which the fresh chicken eggshell membrane still can retain its PSF correlation of more than 65% (Fig. 5a). From the last speckle patterns of the set and its corresponding localized emitters, we re-estimate the PSF. This newly estimated PSF is used to reconstruct a new set of next 50 speckle patterns. The process is continued for all 300 collected stochastic patterns (6 sets) to reconstruct a complete SOSLI image as presented in Fig. 5c. The final image with adaptive SOSLI is super-resolution, much clearer and less noise compared to SOSLI with a static PSF (Fig. 5b). For comparison, the low-resolution images obtained by the phase retrieval algorithm and invasive deconvolution of this object through the chicken eggshell membrane are similar to Fig. 1b-c, respectively. The adaptive SOSLI mitigates the decorrelation problems of dynamic scattering media and allows us to reconstruct a super-resolution image (Fig. 5c) with effective correlation of more than 0.65 (shaded area in Fig. 5a), while the actual correlation reduces to 0.2 during image acquisition. Certainly, the dynamic scattering media degrade image reconstruction quality compared to that of static media due to the artifact in deconvolution using slightly decorrelated PSF. But its resolution is still better than single-shot invasive and non-invasive imaging (Fig. 1b-c). The procedure can continue with more stochastic

pattern acquisition and the membrane is even completely decorrelated, but the effective correlation for adaptive SOSLI still can maintain at more than 65%.

We can further modify the process to be the most adaptive SOSLI for extremely dynamic scattering media where the deconvolution might fail even when using the estimated PSF for immediately next speckle pattern. Here, we can reconstruct the super-resolution image by retrieving every emitter pattern from its speckle autocorrelation with the phase retrieval algorithm and then localization. The deconvolution image (with the PSF estimated from the previous speckle pattern) is only used as the initial guess for phase retrieval algorithm. This is especially important to maintain no-shifting and no-flipping among all retrieved images for superposition. In our demonstration, only 20% correlation of the scattering media between two shots is sufficient to achieve no-shifting and no-flipping in their phase retrieved images. However, phase retrieval algorithm is known for its sensitivity to input parameters and initial guess; though it is rare, we see small shifting but flipping. Phase retrieval algorithm can clean and correct various artifacts in the deconvolution image (initial guess), thus helps localization but it is blind to position errors. And certainly, 20% correlation is enough to identify the flipping direction in the initial guess; and therefore, phase retrieval algorithm does not change it. To further increase the resolution of our most adaptive SOSLI, we can check relative position of the estimated PSF with previous one to shift the retrieved emitter pattern accordingly before superposing for the super-resolution image (supplementary Fig. S8).

Discussion and Conclusion

We would like to highlight the important role of SNR on resolution, the fundamental problem for all computational super-resolution microscopy, including our SOSLI. For conventional super-resolution microscopy with microscope objectives and transparent samples[7-9], all photons from a single emitter go into its diffraction limit spot on the camera, which can be few tens to thousands of pixels depending on magnification and NA. With scattering media, however, the photons are scattered everywhere, forming speckles inside and even outside the camera; in addition, we need multiple speckles to retrieve an image. The SNR is very low with SOSLI and we cannot easily increase it simply by increasing the integration time because we need stochastic nature of blinking emitters from frame to frame. To enhance SNR, beside the requirement of a low noise camera, high photon budget (number of photons per blink per emitter) is a challenging requirement. Ultrabright single fluorophores or quantum emitters could emit at the best 10^4 - 10^6 photons per blink to a camera[38], which is equivalent to 10^1 - 10^3 photons per pixel (PPP) for normal imaging with objective lens and transparent samples. For scattering media, however, this implies much less than 10^{-2} - 10^0 PPP (for a megapixel camera) which is lower than noise floor of the camera. The low photon budget also implies the uncertainty of the captured speckle patterns regardless of noise (supplementary Fig. S9). Such quantum uncertainty is the significant noise source for SOSLI with intermittent emitters. Our simulation (supplementary Fig. S10) for static scattering media and noiseless experiments shows that 11% of success rate for phase

retrieval and localization can be achieved with about 1 PPP. After PSF is estimated, the success rate for deconvolution and localization is very high such as 68% for 0.1 PPP and 100% for 0.45 PPP and above (supplementary Fig. S11). It is understandable that our bottleneck is the phase retrieval algorithm and multi-million photons are required for SOSLI. The future development of inorganic quantum emitters with very high quantum yield and suppressed blinking rate[39] could enable SOSLI in practical applications.

Besides the SNR, other main factors affecting SOSLI's performance are the memory effect region, the sample sparsity, and spectral line width of the emitters. The sample size should be within the memory effect region, which is inverse proportional to the scattering media thickness. While the ratio ($R = L/l$) between media thickness (L) and the mean free path (MFP, l), which is either scattering MFP for scattering regime or transport MFP for diffusion regime, determines how strong the scattering effect is, it does not define how large memory effect region is. SOSLI can be successful with a very large ratio R (i.e. multiple scattering) if L is small (i.e. the MFP is also small). But SOSLI can be easily failed with a small ratio R (i.e. from few to single scattering) if the media is thick (i.e. both L and l are large). Our computational approach starts with phase retrieval algorithm which is known for random artifacts, and we should try several times to get the best results. And certainly, the sample sparsity (less input information) together with a large number of speckles per pattern captured by the camera (more measured signals) helps to improve the autocorrelation estimation and enhance the

performance of phase retrieval algorithm. For the last point, SOSLI relies on incoherent light speckle patterns, which are low contrast if the spectral bandwidth is large. Our 10nm band pass filter certainly helps to improve the speckle contrast from projector's pixels. Several inorganic quantum emitters (such as quantum dots, nanoplatelets) can provide such narrow spectral bandwidth for potential demonstrations.

Demonstration SOSLI at nanometer resolution is desired but requires nanoscale intermittent emitters with a high photon budget. Our demonstration with de-magnifying DMD pixels allows us to illustrate SOSLI closest to actual practice, but we must intentionally reduce the NA of the imaging system to show the super-resolution effect for 1.34μm feature size. We now demonstrate SOSLI with a 3-bright-dot sample which is about 1 mm behind the ground glass. The diameter of each dot is 100 nm. To increase the signal, scattering photons after scattering media are collected by a microscope objective (NA = 0.6) to a camera. There is no aperture in the setup. The scattering angle of ground glass, the field of view and the NA of microscope objective define the overall NA of the SOSLI system. An 1D-piezo stage moves the 3-dot sample randomly within 6 μm horizontal distance. The camera captures speckle pattern at every sample position for SOSLI. The inset of Fig. 6a shows a typical deconvolution image with an estimated PSF. It illustrates the diffraction limit spot of 0.8 μm, implying the overall NA of 0.42 for the SOSLI setup. Figure 6a presents the superposing image of all the diffraction limited deconvolution images, whereas Fig. 6b shows the SOSLI result, which resolves clearly the 100-nm lines with a 400-nm clean gap between them.

Our demonstration with random positions of the 3-dot sample could mimic the random blinking phenomenon of emitters at a certain level, but the relative positions among three dots are unchanged in each frame. With the existing data set, we add several random speckle patterns together to generate new speckle patterns which would be the speckle patterns if 3, or 6, …, or 18 dots were on simultaneously. In each speckle pattern, the relative positions among these dots are random (inset of Fig. 6c). Such generated speckle patterns can be considered as taken from truly stochastic blinking emitters with very high photon budgets. The reconstructed image by SOSLI from these speckle patterns are super resolution with very small artifacts at the gap between two thin lines because there is possibility that two dots within a diffraction limit spot are on simultaneously. Figure 6d presents the intensity profile across the vertical line of the images; SOSLI can resolve the lines at single pixel precision. Compared to the diffraction limit, our SOSLI achieves an 8-fold enhancement which is again currently limited by 100-nm holes in sample fabrication. The image reconstruction process for SOSLI is illustrated in the supplementary video.

In summary, we have demonstrated SOSLI for non-invasive super-resolution imaging through both static (ground glass) and highly dynamic scattering media (fresh chicken eggshell membrane). The camera captures multiple images of scattered light from stochastic emitters behind scattering media, and then our computational approach localizes these emitters non-invasively to reconstruct a super-resolution image. Our experimental results show that SOSLI enhances resolution by a factor of 8 compared to

the diffraction limit, showing 100-nm features with considerably more detail compared to both state-of-the-art invasive and non-invasive imaging through scattering media. Similar to other computational super-resolution techniques, SOSLI's resolution is dictated by SNR which, however, requires very high photon budget to have acceptable SOSLI performance. The adaptive SOSLI allows super-resolution imaging non-invasively through highly dynamic scattering media with decorrelation of up to 80% between two consecutive speckle patterns. Our SOSLI demonstration shows a promising approach for optical imaging through dynamic turbid media, such as biological tissue, with unprecedented clarity.

Method

Scale bar: With the exception of the experiment in Fig. 6, all other experimental results show a scale bar of 10 camera pixels that is equivalent to 65 μm in the imaging plane and 6.5 μm on the object plane (the magnification is 10 in our experiments). However, we do not know the scale bar on the object plane or the magnification of the imaging system in the non-invasive approach because the distance from the object to scattering media is unknown. We can only resolve the sample by angular resolution as presented in Fig. 3 & 6, which is the same for both imaging and object plane.

For experiment in Fig. 6, the scale bar is calculated based on the fabricated ground truth sample with exact distance among 3 dots. This approach provides better accuracy than calculation based on the camera pixel size and imaging optics due to the involvement

of microscope objective in the speckle imaging side.

Scattering media: The static scattering media are 120 grit ground glass diffusers from Thorlabs or Edmund. The memory effect region is 15 mrad, which implies the effective thickness of the scattering media is 18 μm (Ref. 27). The chicken eggshell membrane has similar effective thickness when fresh, then this increases when dried.

Nanoscale sample: A gold film, 250 nm thick, was deposited on a microscope glass slide. Focus ion beam (FIB) technique was used to create three 100-nm holes in the gold film. The 3-hole sample was illuminated from behind by a focused green LED through an objective lens.

Data processing: In all experiments, the resolution of the raw camera images is 2560×2160 pixels. We crop them into a resolution of 2048×2048 pixels for implementation of all the mentioned techniques in this work. The final reconstructed images are cropped to a square window with dimensions ranging between 75×75 pixels and 200×200 pixels (depending on the imaged object dimensions). Algorithms are developed in Matlab and run on a normal PC (Intel Core i7, 16 GB memory). A typical procedure for SOSLI with 300 speckle patterns takes 2-3 minutes.

Data and code availability: The sample data and the code are available at the public repositories as: https://figshare.com/s/f438c15c3beee10545de

Supplementary video: The introduction video together with the recorded video on super-resolution image reconstruction by SOSLI is available at

https://youtu.be/k8CPMvidfuo (currently not searchable on internet; the video will be made public together with manuscript publication later)

Funding

The research is financially supported by Ministry of Education – Singapore (MOE): MOE-AcRF Tier-1 (MOE2019-T1-002-087), and Nanyang Technological University Singapore (NTU).

Acknowledgements

The authors specially thank Professor Nikolay I. Zheludev at University of Southampton and Nanyang Technological University, Singapore together with Professor Sylvain Gigan and his research group at Laboratoire Kastler Brossel, Sorbonne Université, École Normale Supérieure–Paris Sciences et Lettres (PSL) Research University, Paris, France for great discussions and providing suggestions for improvement. We would like to thank Vinh Tran, Dr. Dayan Li, Dr. Dongliang Tang, and Dr. Huy Lam at NTU Singapore for fruitful discussions and useful feedbacks. We would like to thank Dr. Philip Anthony Surman for proof reading.

Author contributions

C.D. initiated the idea. S.K.S. developed the Matlab code and performed the numerical simulations. C.D., D.W. and S.K.S. designed the initial experiments. D.W. performed the experiments using a projector with S.K.S.'s participation. X.Z and C.D.

performed the experiments for 100-nm samples. G. A. fabricated 100-nm samples. C.D. and D.W. wrote the manuscript with S.K.S.'s contributions. All authors discussed, analyzed and took responsibility for the results and revised the manuscript. C.D. supervised and contributed to all aspects of research.

References

1. Schermelleh, L. *et al.* Super-resolution microscopy demystified. *Nature Cell Biology* **21**, 72-84, (2019).

2. Neef, J. *et al.* Quantitative optical nanophysiology of Ca2+ signaling at inner hair cell active zones. *Nature Communications* **9**, 290, (2018).

3. Pujals, S., Feiner-Gracia, N., Delcanale, P., Voets, I. & Albertazzi, L. Super-resolution microscopy as a powerful tool to study complex synthetic materials. *Nature Reviews Chemistry* **3**, 68-84, (2019).

4. Hell, S. W. & Wichmann, J. Breaking the diffraction resolution limit by stimulated emission: stimulated-emission-depletion fluorescence microscopy. *Opt Lett* **19**, 780-782, (1994).

5. Vicidomini, G., Bianchini, P. & Diaspro, A. STED super-resolved microscopy. *Nature Methods* **15**, 173, (2018).

6. Hell, S. W. Toward fluorescence nanoscopy. *Nature Biotechnology* **21**, 1347-1355, (2003).

7. Betzig, E. Proposed method for molecular optical imaging. *Opt Lett* **20**, 237-239, (1995).

8. Betzig, E. *et al.* Imaging Intracellular Fluorescent Proteins at Nanometer Resolution. *Science* **313**, 1642-1645, (2006).

9. Balzarotti, F. *et al.* Nanometer resolution imaging and tracking of fluorescent molecules with minimal photon fluxes. *Science* **355**, 606-612, (2017).

10. Turcotte, R. *et al.* Dynamic super-resolution structured illumination imaging in the living brain. *Proceedings of the National Academy of Sciences* **116**, 9586-9591, (2019).

11. Tenne, R. *et al.* Super-resolution enhancement by quantum image scanning

microscopy. *Nat Photonics* **13**, 116-122, (2019).

12. Kaldewey, T. *et al.* Far-field nanoscopy on a semiconductor quantum dot via a rapid-adiabatic-passage-based switch. *Nat Photonics* **12**, 68-72, (2018).

13. Goodman, J. W. *Speckle Phenomena in Optics: Theory and Applications*. (Roberts & Company, 2007).

14. Kang, S. *et al.* Imaging deep within a scattering medium using collective accumulation of single-scattered waves. *Nat Photonics* **9**, 253, (2015).

15. Siddiqui, M. *et al.* High-speed optical coherence tomography by circular interferometric ranging. *Nat Photonics* **12**, 111-116, (2018).

16. Hoover, E. E. & Squier, J. A. Advances in multiphoton microscopy technology. *Nat Photonics* **7**, 93, (2013).

17. Ntziachristos, V. Going deeper than microscopy: the optical imaging frontier in biology. *Nature Methods* **7**, 603, (2010).

18. Čižmár, T., Mazilu, M. & Dholakia, K. In situ wavefront correction and its application to micromanipulation. *Nat Photonics* **4**, 388, (2010).

19. Horstmeyer, R., Ruan, H. & Yang, C. Guidestar-assisted wavefront-shaping methods for focusing light into biological tissue. *Nat Photonics* **9**, 563, (2015).

20. Judkewitz, B., Wang, Y. M., Horstmeyer, R., Mathy, A. & Yang, C. Speckle-scale focusing in the diffusive regime with time reversal of variance-encoded light (TROVE). *Nat Photonics* **7**, 300, (2013).

21. Si, K., Fiolka, R. & Cui, M. Fluorescence imaging beyond the ballistic regime by ultrasound-pulse-guided digital phase conjugation. *Nat Photonics* **6**, 657, (2012).

22. Choi, Y. *et al.* Overcoming the Diffraction Limit Using Multiple Light Scattering in a Highly Disordered Medium. *Physical Review Letters* **107**, 023902, (2011).

23. Chaigne, T. *et al.* Controlling light in scattering media non-invasively using the photoacoustic transmission matrix. *Nat Photonics* **8**, 58, (2013).

24. Osnabrugge, G., Horstmeyer, R., Papadopoulos, I. N., Judkewitz, B. & Vellekoop, I. M. Generalized optical memory effect. *Optica* **4**, 886-892, (2017).

25. Freund, I., Rosenbluh, M. & Feng, S. Memory Effects in Propagation of Optical Waves through Disordered Media. *Physical Review Letters* **61**, 2328-2331, (1988).

26. Tang, D., Sahoo, S. K., Tran, V. & Dang, C. Single-shot large field of view imaging with scattering media by spatial demultiplexing. *Applied Optics* **57**, 7533-7538, (2018).

27. Sahoo, S. K., Tang, D. & Dang, C. Single-shot multispectral imaging with a monochromatic camera. *Optica* **4**, 1209-1213, (2017).

28. Edrei, E. & Scarcelli, G. Memory-effect based deconvolution microscopy for super-resolution imaging through scattering media. *Scientific reports* **6**, 33558, (2016).

29. Lyons, A. *et al.* Computational time-of-flight diffuse optical tomography. *Nat Photonics*, (2019).

30. Eggebrecht, A. T. *et al.* Mapping distributed brain function and networks with diffuse optical tomography. *Nat Photonics* **8**, 448, (2014).

31. O'Toole, M., Lindell, D. B. & Wetzstein, G. Confocal non-line-of-sight imaging based on the light-cone transform. *Nature* **555**, 338, (2018).

32. Bertolotti, J. *et al.* Non-invasive imaging through opaque scattering layers. *Nature* **491**, 232-234, (2012).

33. Katz, O., Heidmann, P., Fink, M. & Gigan, S. Non-invasive single-shot imaging through scattering layers and around corners via speckle correlations. *Nat Photon* **8**, 784-790, (2014).

34. Okamoto, Y., Horisaki, R. & Tanida, J. Noninvasive three-dimensional imaging through scattering media by three-dimensional speckle correlation. *Opt Lett* **44**, 2526-2529, (2019).

35. Huang, B., Wang, W., Bates, M. & Zhuang, X. Three-Dimensional Super-Resolution Imaging by Stochastic Optical Reconstruction Microscopy. *Science* **319**, 810-813, (2008).

36. Rust, M. J., Bates, M. & Zhuang, X. Sub-diffraction-limit imaging by stochastic optical reconstruction microscopy (STORM). *Nature Methods* **3**, 793-796, (2006).

37. Li, D., Sahoo, S. K., Lam, H. Q., Wang, D. & Dang, C. Non-invasive optical focusing inside strongly scattering media with linear fluorescence. *Applied Physics Letters* **116**, 241104, (2020).

38. Vaughan, J. C., Jia, S. & Zhuang, X. Ultrabright photoactivatable fluorophores created by reductive caging. *Nature Methods* **9**, 1181-1184, (2012).

39. Lane, L. A., Smith, A. M., Lian, T. & Nie, S. Compact and Blinking-

Suppressed Quantum Dots for Single-Particle Tracking in Live Cells. *The Journal of Physical Chemistry B* **118**, 14140-14147, (2014).

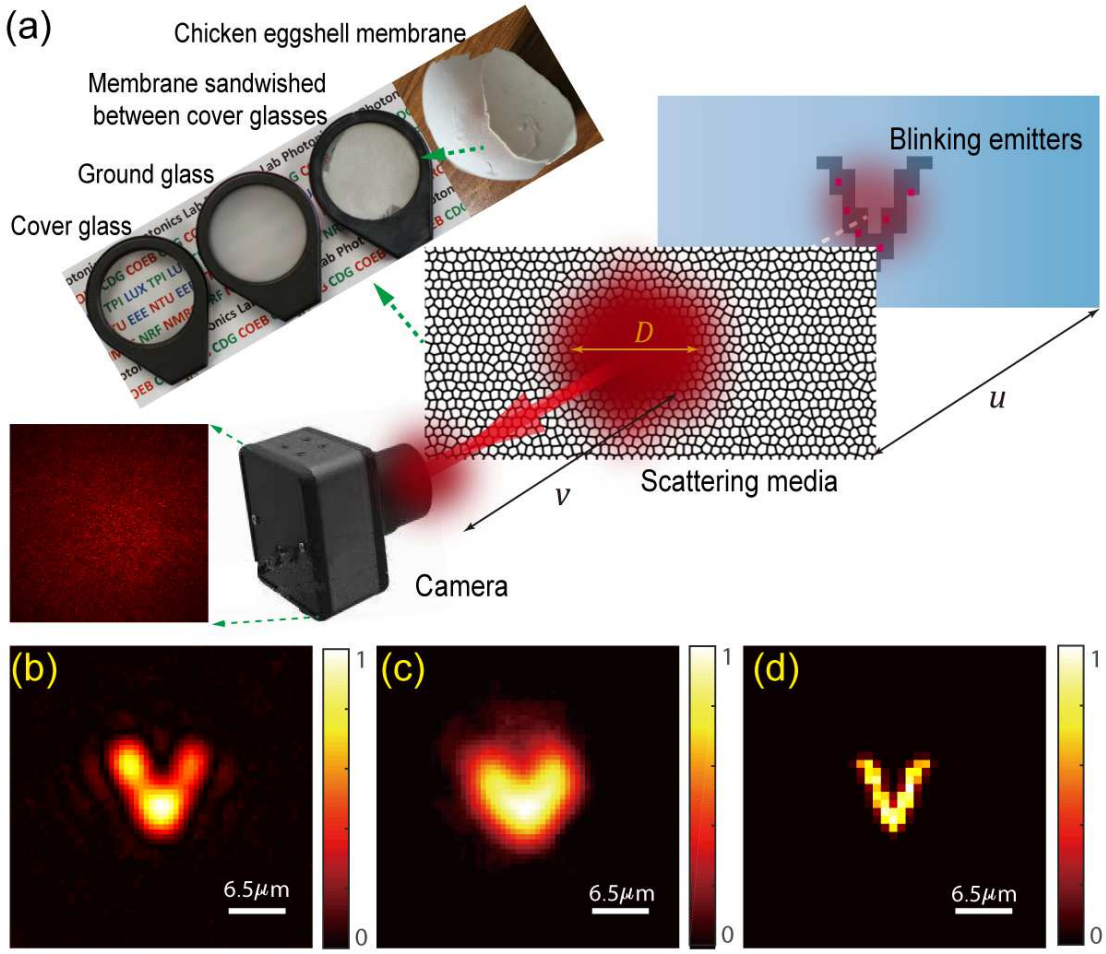

Figure 1. Super-resolution imaging through scattering media with SOSLI in comparison to other imaging techniques. (a) Schematic of SOSLI where incoherent light from blinking emitters hidden behind various scattering media is scattered and then captured by a camera. **(b-d)** Experimental demonstrations of the current state-of-art invasive imaging, non-invasive imaging, and our super-resolution SOSLI, respectively, through the same scattering medium in the identical experimental setup.

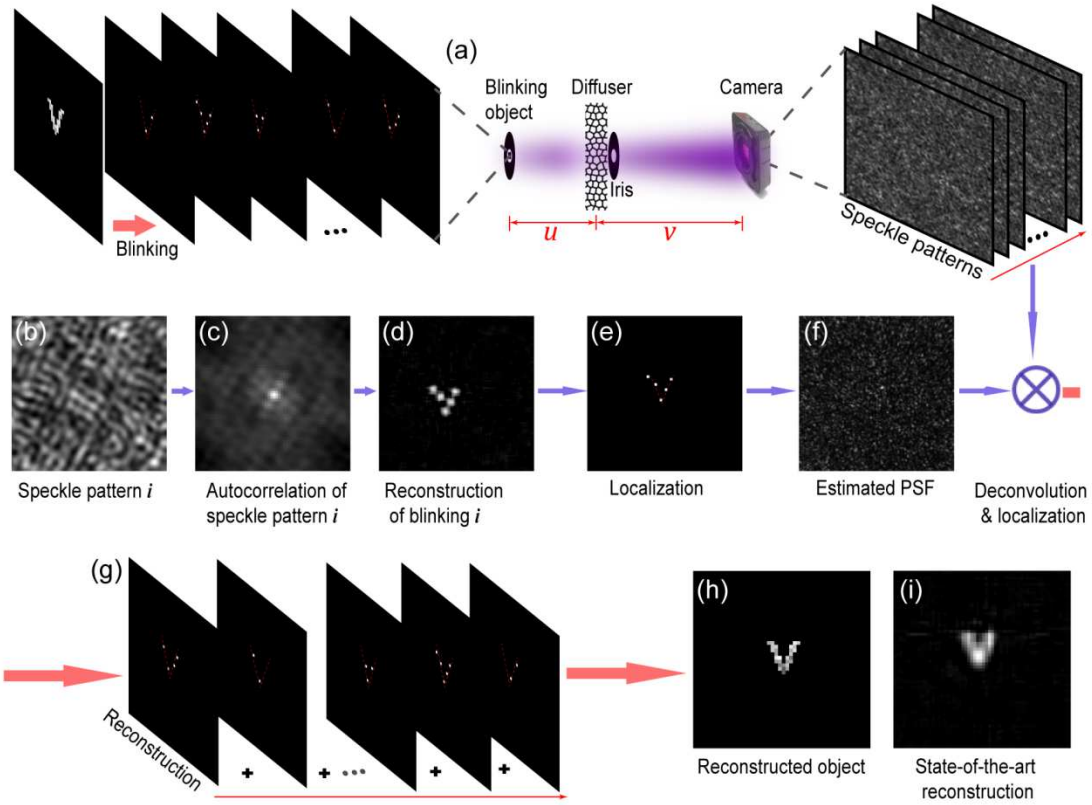

Figure 2. Principle and simulation results of SOSLI. (a) Object constitutes many intermittent emitters behind an optical diffuser; the iris defines the optical aperture of the imaging system and the camera captures speckle patterns. **(b)** A small portion of a typical speckle pattern. **(c)** Autocorrelation of the speckle pattern is similar to that of the emitter pattern. **(d)** A retrieved image from its autocorrelation. **(e)** Localized emitters from the retrieved image. **(f)** Estimated PSF' from the localized emitter image (e) and its corresponding speckle pattern (b). **(g)** A series of localized emitter images by deconvolution of the speckle patterns with the estimated PSF'. **(h)** A reconstructed image with a sub-diffraction-limit resolution by superposing all the individual localized emitter images. **(i)** A retrieved image from a single-shot speckle pattern when all emitters are on, i.e. the current state-of-art non-invasive imaging scheme[33].

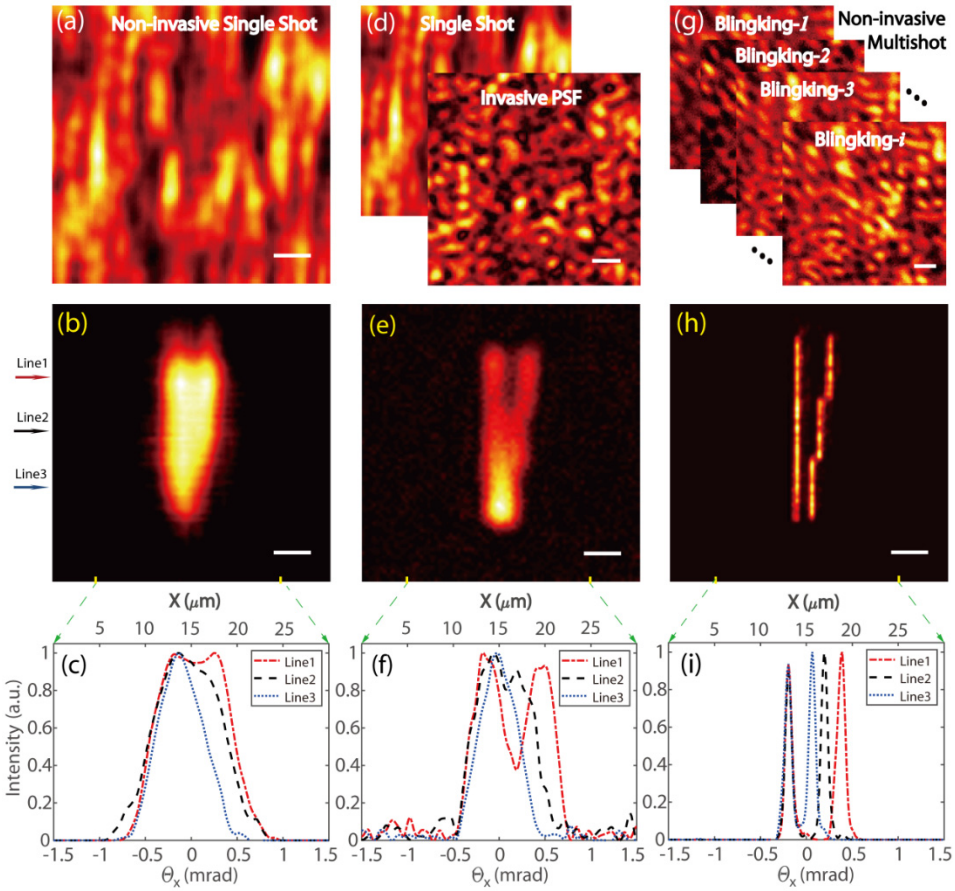

Figure 3. Experimental results of imaging through a ground glass diffuser with different techniques. (a) Non-invasive single-shot speckle pattern for phase retrieval algorithm **(b-c)** Phase retrieved image and its intensity profile, respectively. **(d)** Invasively measured PSF and single-shot speckle pattern for deconvolution imaging. **(e-f)** Deconvolution image and its intensity profile, respectively. **(g)** Non-invasive speckle patterns from a stochastic sample for SOSLI **(h-i)** Non-invasive super-resolution imaging by our SOSLI and its intensity profile, respectively. Three arrows on the left indicate the three lines for cross-sectional intensity curves in figure c, f, i. Scale bars: 10 camera pixels, equivalent to 6.5 μm on the object plane.

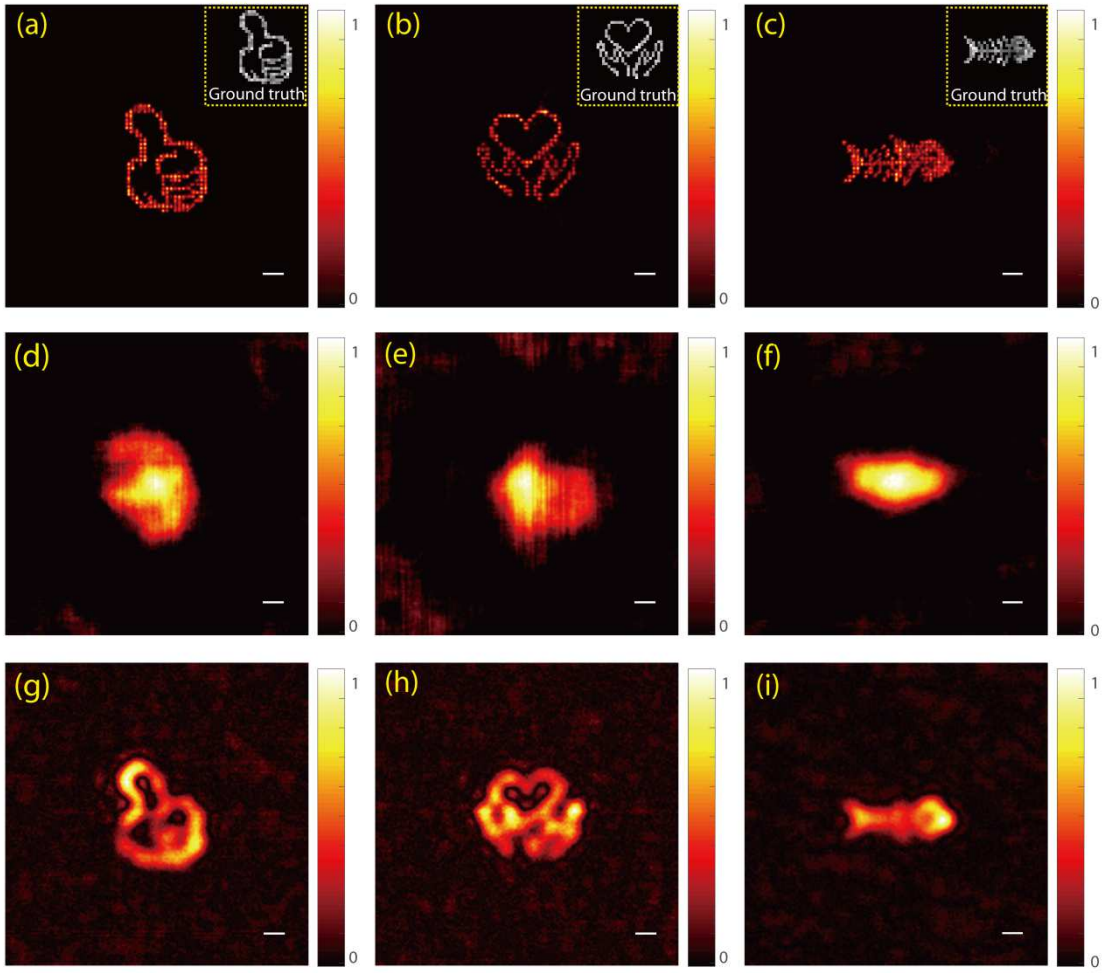

Figure 4. Experimental demonstration of three techniques for imaging several complex objects hidden behind a ground glass diffuser. (a-c) Our SOSLI approach for non-invasive super-resolution imaging. Insets are ground truth objects. **(d-f)** Non-invasive imaging retrieved from autocorrelation of a single speckle pattern for the ground truth samples in the insets of a, b and c, respectively. **(g-i)** Invasive imaging with an invasively measured PSF and deconvolution approach for the ground truth samples in the insets of a, b and c, respectively. Scale bars: 6.5 μm.

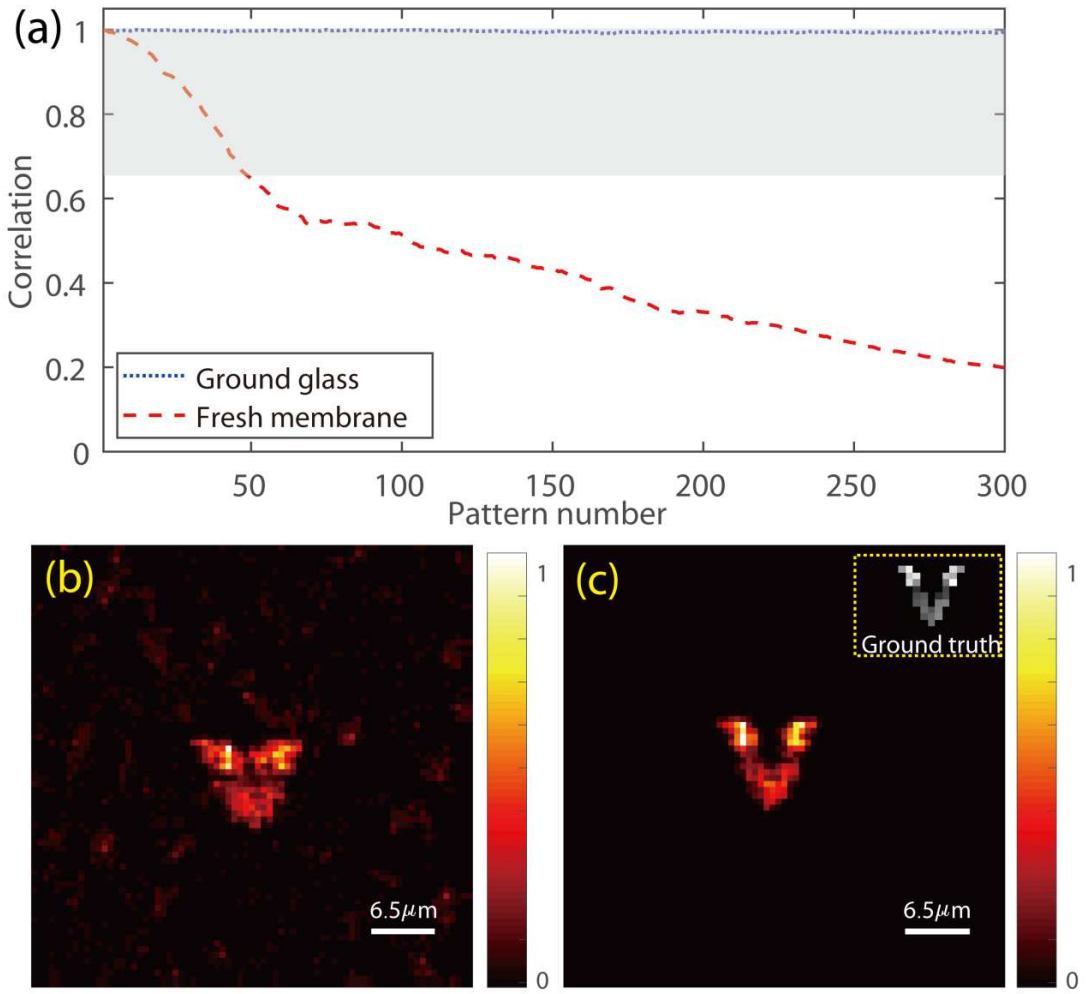

Figure 5. Experimental demonstration of non-invasive super-resolution imaging through a fresh chicken eggshell membrane by SOSLI. **(a)** Speckle correlation of PSFs at different measurement time for the static scattering medium (ground glass) and the dynamic one (the fresh chicken eggshell membrane). **(b)** The reconstructed image by SOSLI with a single estimated PSF. **(c)** The reconstructed image by SOSLI with adaptive PSF estimation.

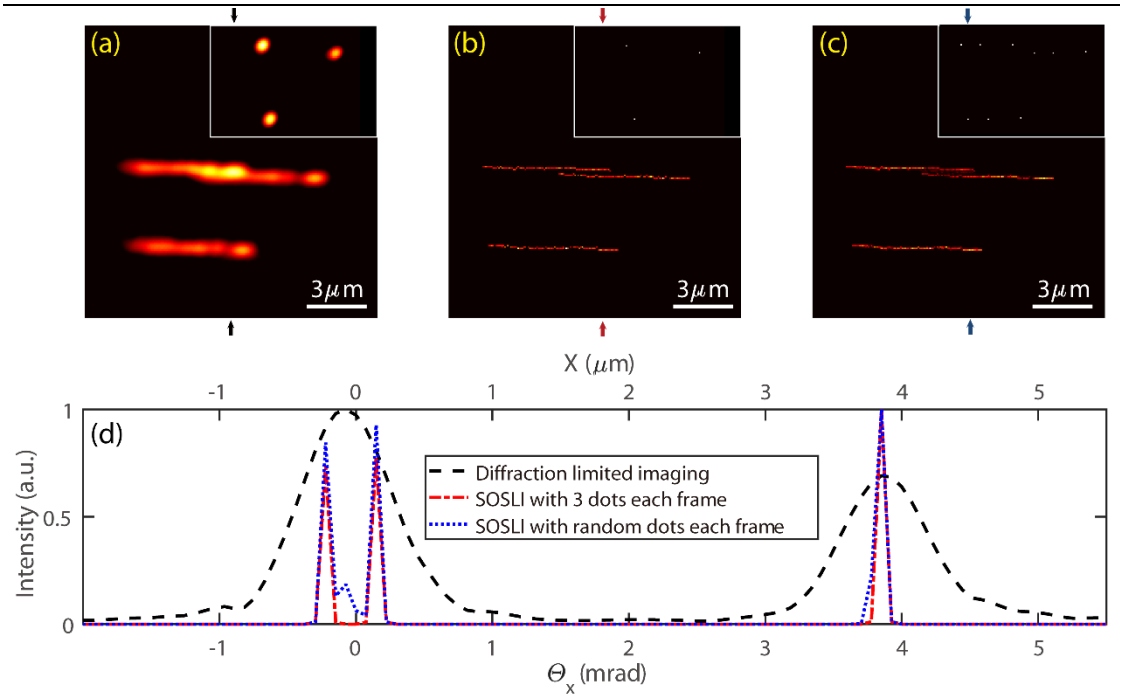

Figure 6: SOSLI demonstration with sub-wavelength resolution. a) Superposing multiple low-resolution images of a 3-dot sample at various random positions; **inset:** a typical low-resolution image. **b)** The SOSLI result of a 3-dot sample at various random positions; **inset:** a typical localization image. **c)** The SOSLI image with randomly appearing dots; **inset:** a typical localization image. **d)** Intensity profile across the vertical line of three images (corresponding to the colored arrows on the figure a, b, c).

Figures

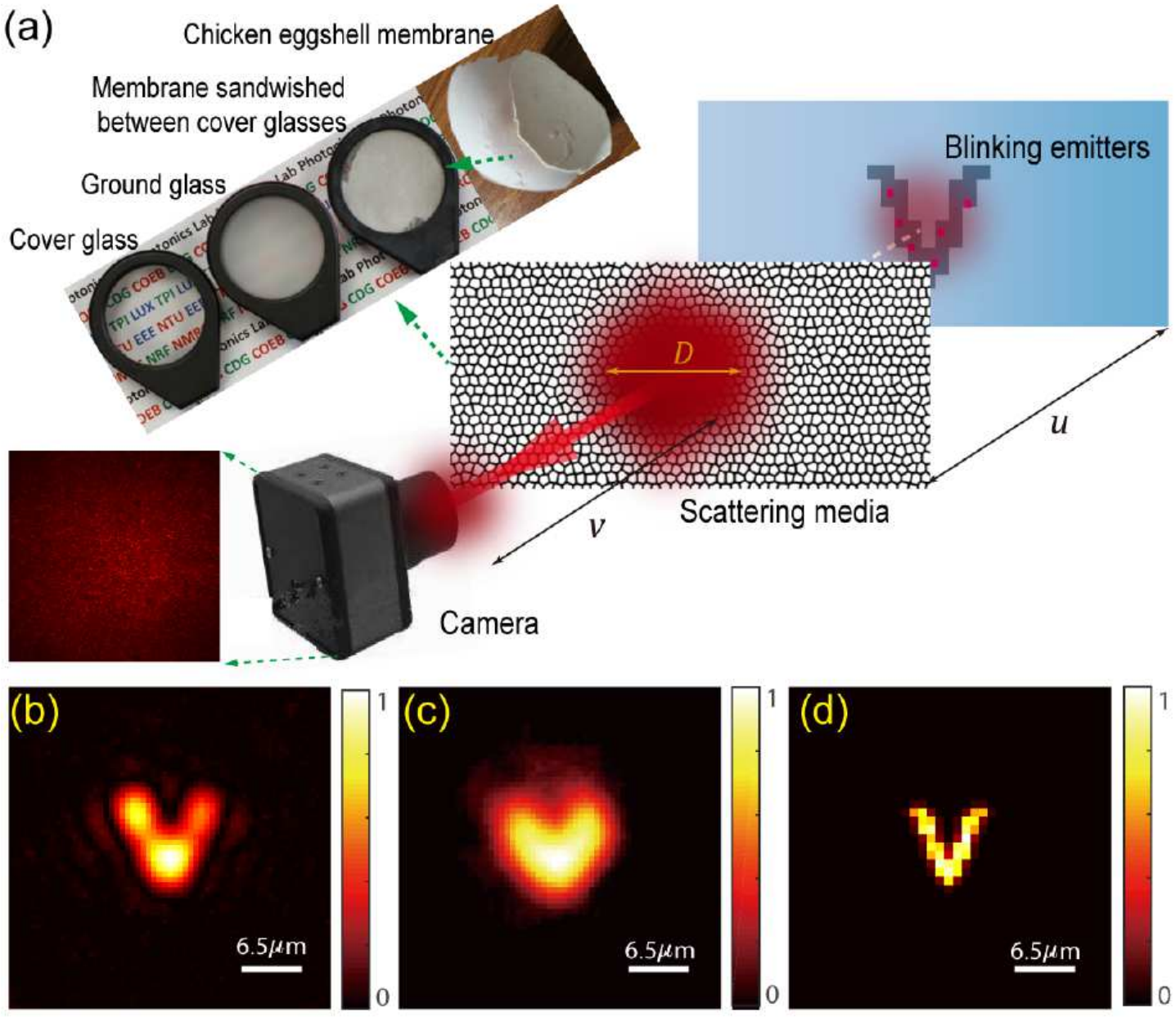

Figure 1

Super-resolution imaging through scattering media with SOSLI in comparison to other imaging techniques. (a) Schematic of SOSLI where incoherent light from blinking emitters hidden behind various scattering media is scattered and then captured by a camera. (b-d) Experimental demonstrations of the current state-of-art invasive imaging, non-invasive imaging, and our super-resolution SOSLI, respectively, through the same scattering medium in the identical experimental setup.

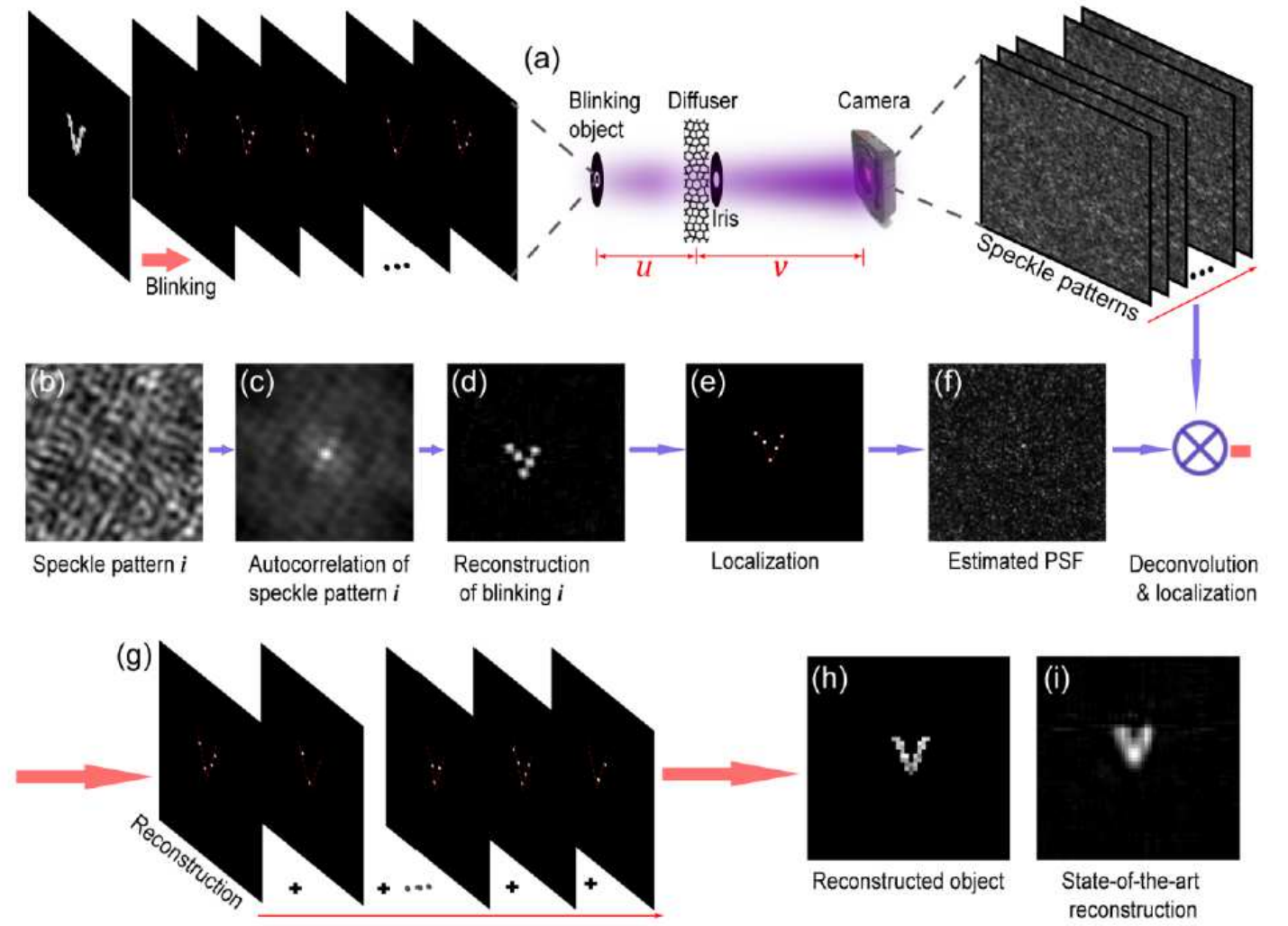

Figure 2

Principle and simulation results of SOSLI. (a) Object constitutes many intermittent emitters behind an optical diffuser; the iris defines the optical aperture of the imaging system and the camera captures speckle patterns. (b) A small portion of a typical speckle pattern. (c) Autocorrelation of the speckle pattern is similar to that of the emitter pattern. (d) A retrieved image from its autocorrelation. (e) Localized emitters from the retrieved image. (f) Estimated PSF' from the localized emitter image (e) and its corresponding speckle pattern (b). (g) A series of localized emitter images by deconvolution of the speckle patterns with the estimated PSF'. (h) A reconstructed image with a sub-diffraction-limit resolution by superposing all the individual localized emitter images. (i) A retrieved image from a single-shot speckle pattern when all emitters are on, i.e. the current state-of-art non-invasive imaging scheme33.

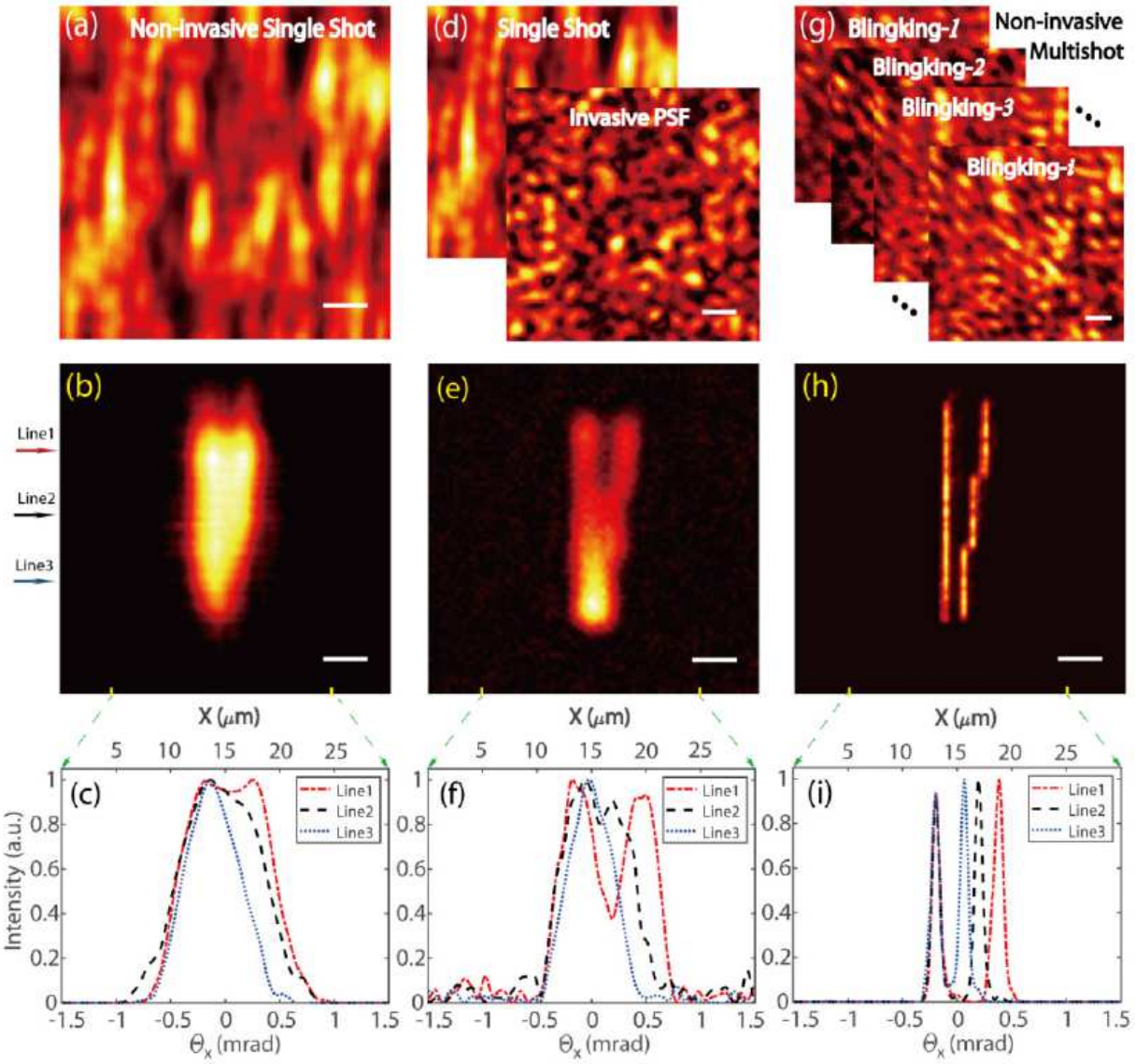

Figure 3

Experimental results of imaging through a ground glass diffuser with different techniques. (a) Non-invasive single-shot speckle pattern for phase retrieval algorithm (b-c) Phase retrieved image and its intensity profile, respectively. (d) Invasively measured PSF and single-shot speckle pattern for deconvolution imaging. (e-f) Deconvolution image and its intensity profile, respectively. (g) Non-invasive speckle patterns from a stochastic sample for SOSLI (h-i) Non-invasive superresolution imaging by our SOSLI and its intensity profile, respectively. Three arrows on the left indicate the three lines for cross-sectional intensity curves in figure c, f, i. Scale bars: 10 camera pixels, equivalent to 6.5 μm on the object plane.

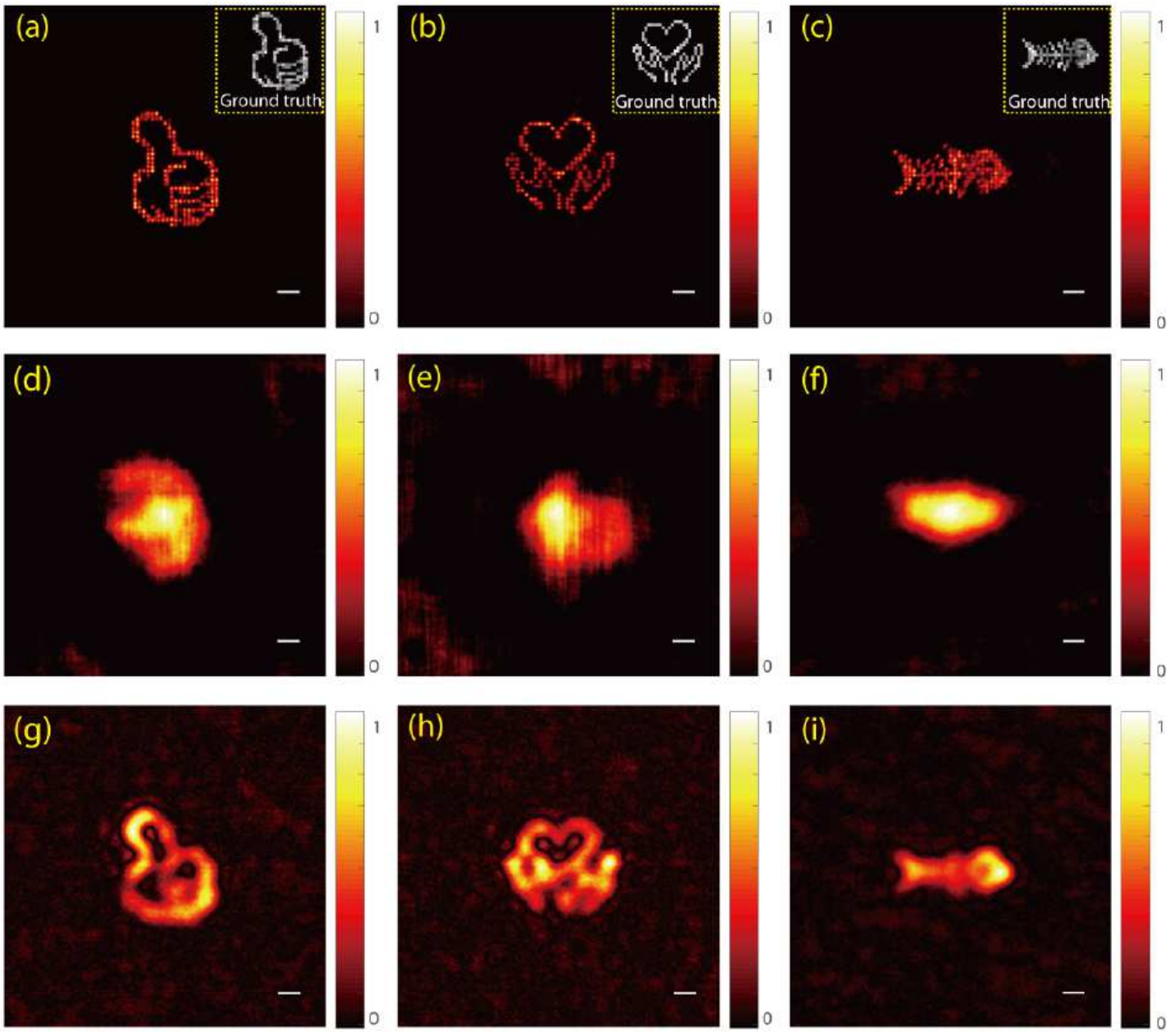

Figure 4

Experimental demonstration of three techniques for imaging several complex objects hidden behind a ground glass diffuser. (a-c) Our SOSLI approach for non-invasive super-resolution imaging. Insets are ground truth objects. (d-f) Noninvasive imaging retrieved from autocorrelation of a single speckle pattern for the ground truth samples in the insets of a, b and c, respectively. (g-i) Invasive imaging with an invasively measured PSF and deconvolution approach for the ground truth samples in the insets of a, b and c, respectively. Scale bars: 6.5 μm.

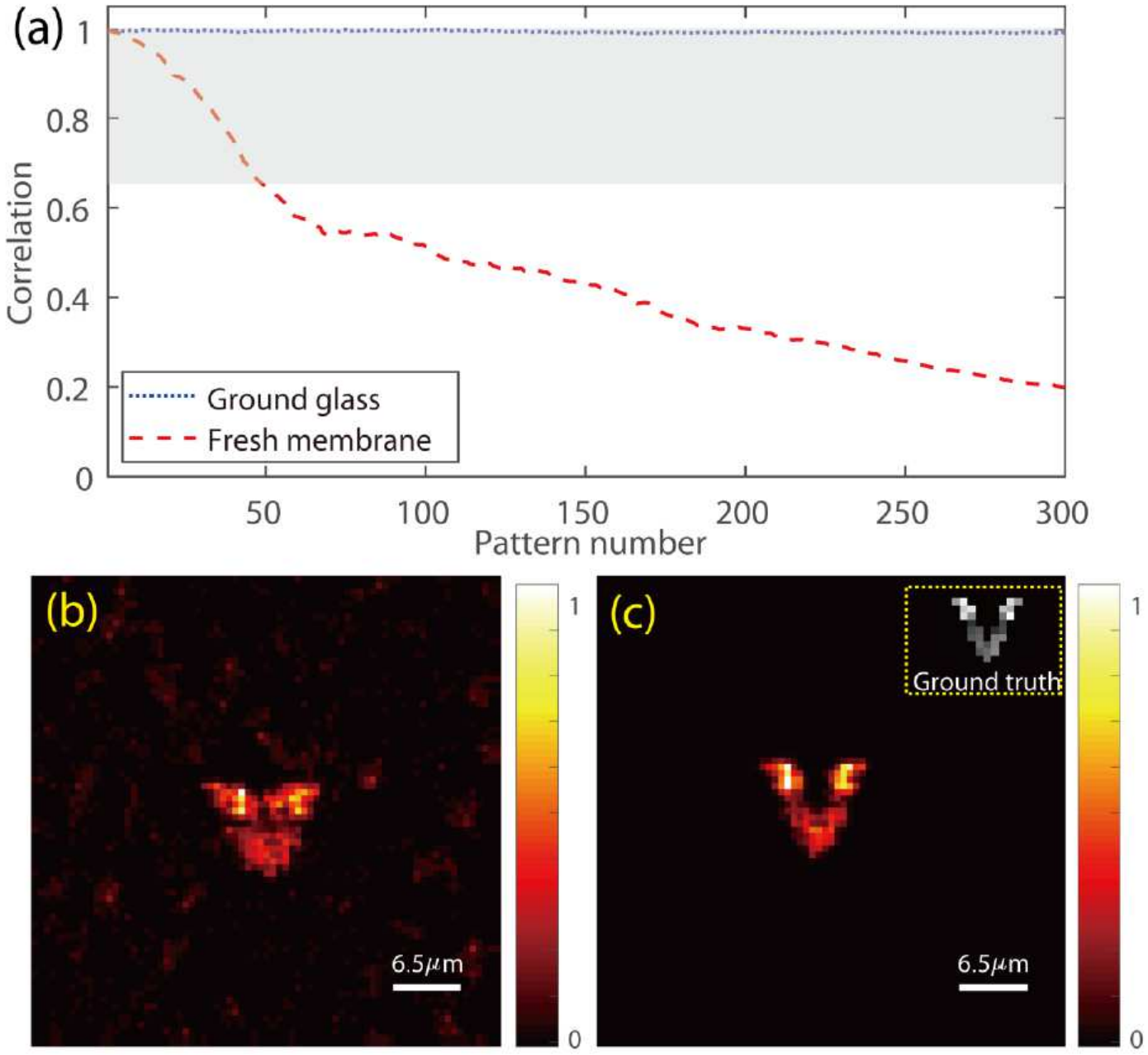

Figure 5

Experimental demonstration of non-invasive super-resolution imaging through a fresh chicken eggshell membrane by SOSLI. (a) Speckle correlation of PSFs at different measurement time for the static scattering medium (ground glass) and the dynamic one (the fresh chicken eggshell membrane). (b) The reconstructed image by SOSLI with a single estimated PSF. (c) The reconstructed image by SOSLI with adaptive PSF estimation.

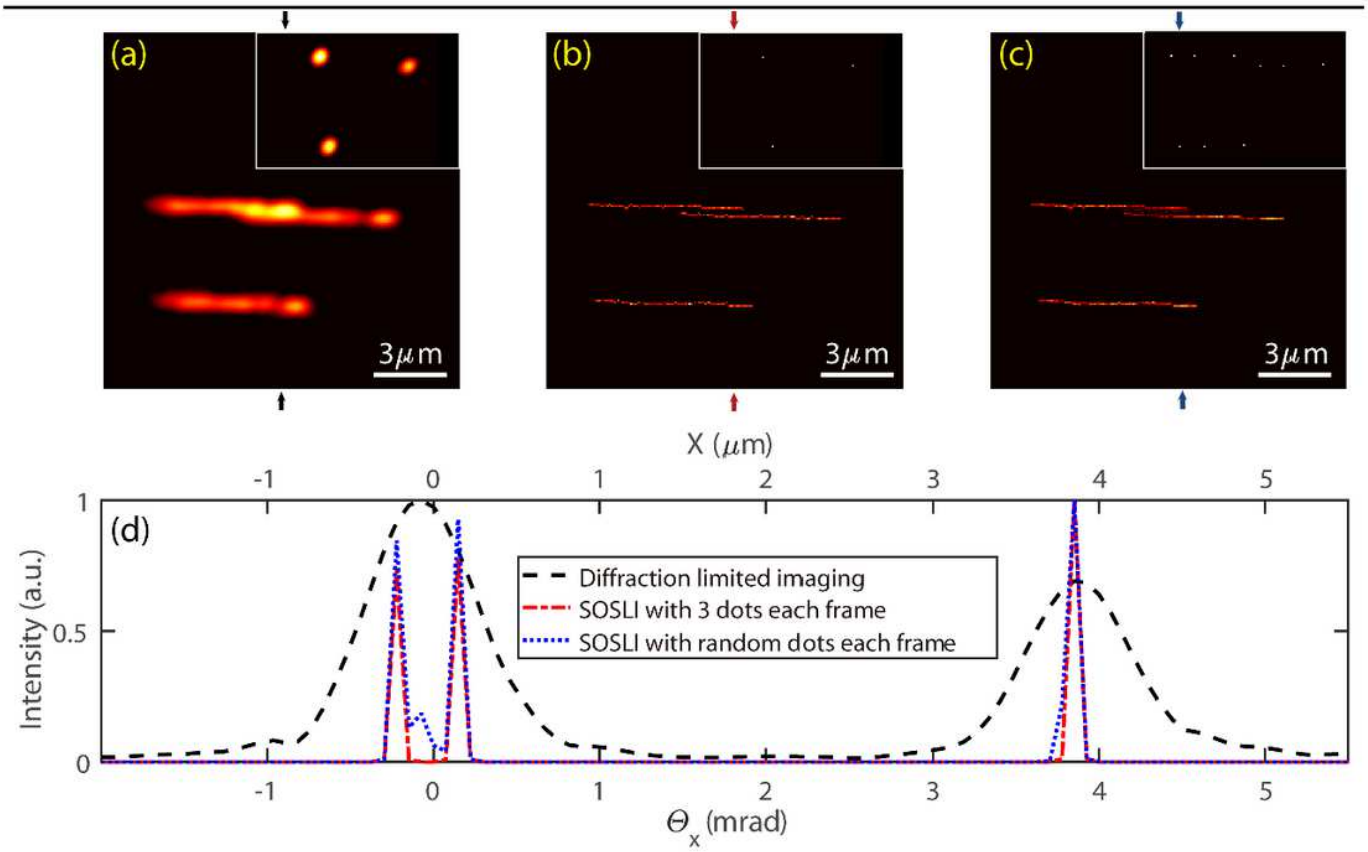

Figure 6

SOSLI demonstration with sub-wavelength resolution. a) Superposing multiple low-resolution images of a 3-dot sample at various random positions; inset: a typical low-resolution image. b) The SOSLI result of a 3-dot sample at various random positions; inset: a typical localization image. c) The SOSLI image with randomly appearing dots; inset: a typical localization image. d) Intensity profile across the vertical line of three images (corresponding to the colored arrows on the figure a, b, c).

Supplementary Files

This is a list of supplementary files associated with this preprint. Click to download.

- SOSLIsupplementarymaterialV6.pdf